

Supporting Information

Activity of Sulfonium Bisphosphonates on Tumor Cell Lines

by

Yonghui Zhang[†], Michael P. Hudock[§], Kilannin Krysiak[†],
Rong Cao[§], Kyle Bergant[†], Fenglin Yin[§], Annette Leon[§] and Eric Oldfield^{†,§,*}

[†]Department of Chemistry,
University of Illinois at Urbana-Champaign,
600 South Mathews Avenue, Urbana, Illinois 61801

and

[§]Center for Biophysics and Computational Biology,
University of Illinois at Urbana-Champaign,
607 South Mathews Avenue, Urbana, Illinois 61801

Table of Contents

Supporting Methods	S3-S4
Supporting Figures	S5-S8
Supporting Tables	S9-S25
Microanalysis Data	S9
Human FPPS and molecular diameter	S11
2D-QSAR output	S12-S16
Hologram QSAR results.....	S17
CoMSIA results	S18-S25
References	S26

Supporting Methods:

QSAR Descriptors: In order to provide sufficient granularity, sub-divided van der Waals surface area descriptors¹ (as implemented in MOE) were utilized in the molar refractivity and positive charge terms, as opposed to whole molecule-based descriptors. Subdivided surface area descriptors map specific molecular properties to a fraction of the van der Waals surface of the molecule², so for example, a whole molecule formal charge descriptor would report back the net charge of the entire molecule, whereas a sub-divided surface area descriptor for charge would compute total surface area for ranges of charge (i.e. $0.10 < q < 0.15$). Although molecular descriptors, such as those described, do not provide explicit feature locations in three-dimensional space, they are often more than sufficient to provide a “fingerprint” and point of comparison between homologous series of compounds. Specifically, in our case, molar refractivity and partial positive charge descriptors were handled in this manner.

Human FPPS inhibition. Human FPPS was expressed and purified as described previously³. Human FPPS assays were carried out using 96 well plates with 200 μL reaction mixture in each well. The condensation of geranyl diphosphate and isopentenyl diphosphate was monitored by a continuous spectrophotometric assay for phosphate releasing enzymes. The reaction buffer contained 50 mM Tris-HCl, 1 mM MgCl₂, at pH 7.4. The compounds investigated were pre-incubated with the enzyme for 30 minutes at 20°C. The IC₅₀ values were obtained by fitting the inhibition data to a normal dose-response curve using Origin 6.1 (OriginLab Corporation, Northampton, MA, www.OriginLab.com).

Crystallization and x-ray data collection for human FPPS bisphosphonate complex. Crystals of human FPPS complexed with Mg and **43** were obtained based on the methods described by Kavanagh *et al.*³, with slight modification. FPPS was incubated with 2.5 mM bisphosphonate and 2.5

mM MgCl₂ overnight on ice before setting up the drops. Crystals were grown at room temperature in sitting drops by mixing 2 µL of protein solution with 1 µL of precipitant, which consisted of 40% (v/v) of either polyethylene glycol 2,000 or 4,000 and 0.1 M phosphate/citrate buffer, pH 4.2. Diffraction data were obtained at 100 K using an ADSC Q315 CCD detector at the Brookhaven National Synchrotron Light Source, beamline X29 ($\lambda=1.1\text{ \AA}$).

Crystallization and x-ray data collection of *T.brucei* FPPS bisphosphonate complex. Crystallization was carried out essentially as reported previously by Mao *et al.*⁴ with **43** used as the inhibitor. Diffraction data were obtained at 100 K using an ADSC Q4 CCD detector at the Brookhaven National Synchrotron Light Source beamline X8C ($\lambda=1.1\text{ \AA}$).

Structure determination of human FPPS bisphosphonate complex. For structure determination, the human FPPS structure (1YV5)³ minus the risedronate ligand was used as a search model using the molecular replacement method. Rigid body refinement was applied to the model obtained using AMoRe⁵. The crystal structure was then further refined by using Shelxl-97⁶, with bisphosphonate densities readily identified. Rebuilding and fitting the ligand in the 2Fo-Fc electron density map was carried out by using the program O⁷.

Structure determination of *T.brucei* FPPS-bisphosphonate complex. The crystal structure of the *T.brucei* FPPS bisphosphonate complex was determined by using the molecular replacement method using the program AMoRe⁵. The previously solved *T.brucei* FPPS structure (2EWG)⁸ minus the minodronate ligand was used as a starting model. The densities of the ligands were readily identified. After iterative rounds of refinement using CNS⁹ and rebuilding and ligand fitting using Coot¹⁰, the structures had the final refinement statistics shown in Table 4 in the text. As expected the refinement statistics are better than those of the human enzyme, due to the lower resolution of the human FPPS dataset.

Supporting Figures:

Figure S1: Experimental and predicted activity correlation matrix. Correlation between data sets represented as an R value. Experimental tumor cell activity and CoMSIA modeling results, both alignments, all three lines shown.

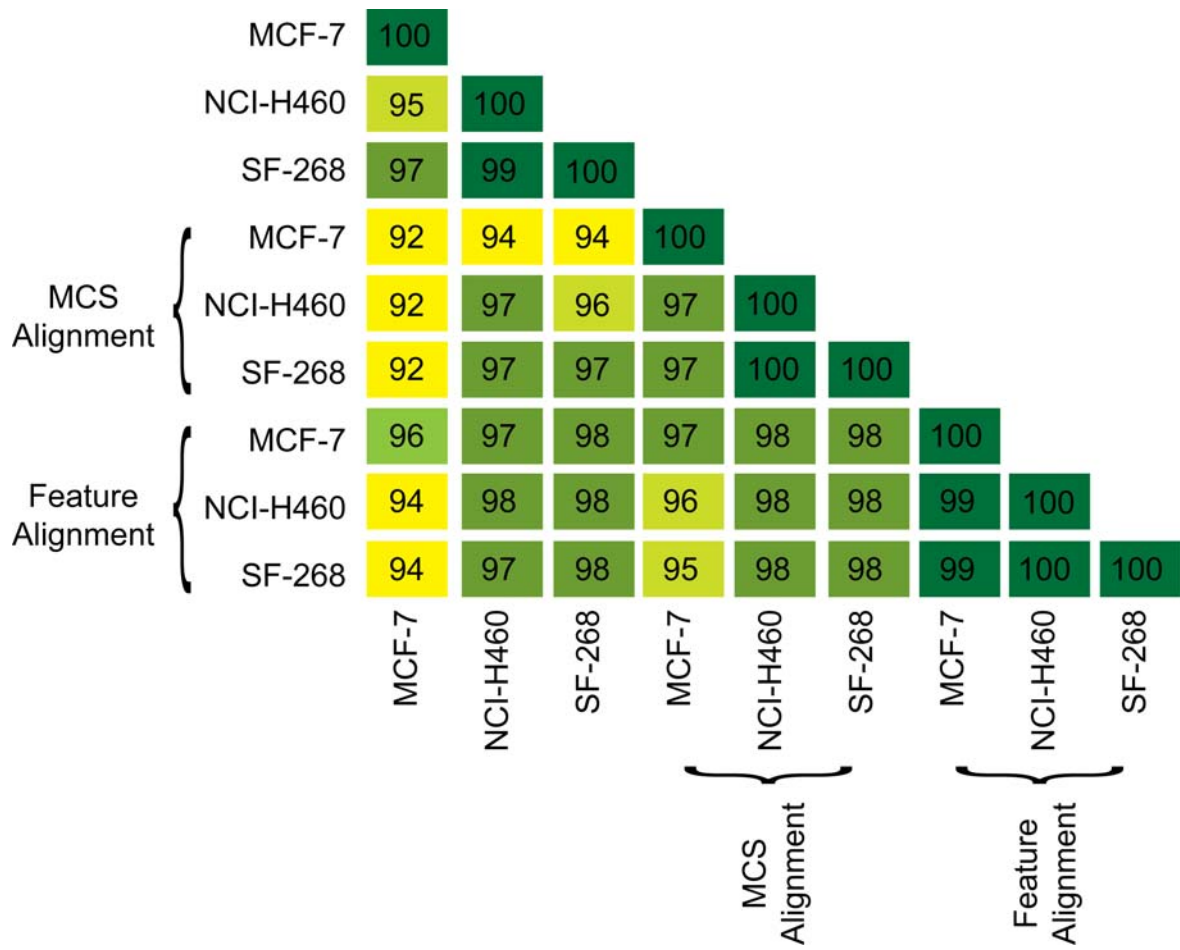


Figure S2: Molecular Descriptor QSAR results for MCF-7 and SF-268 cell lines showing overall good correlation between experimental and predicted pIC_{50} ($r^2 = 0.82$ and 0.78 respectively) ($\text{pIC}_{50} = -\log_{10}[\text{IC}_{50} \text{ M}]$) (● = training set, ○ = test set).

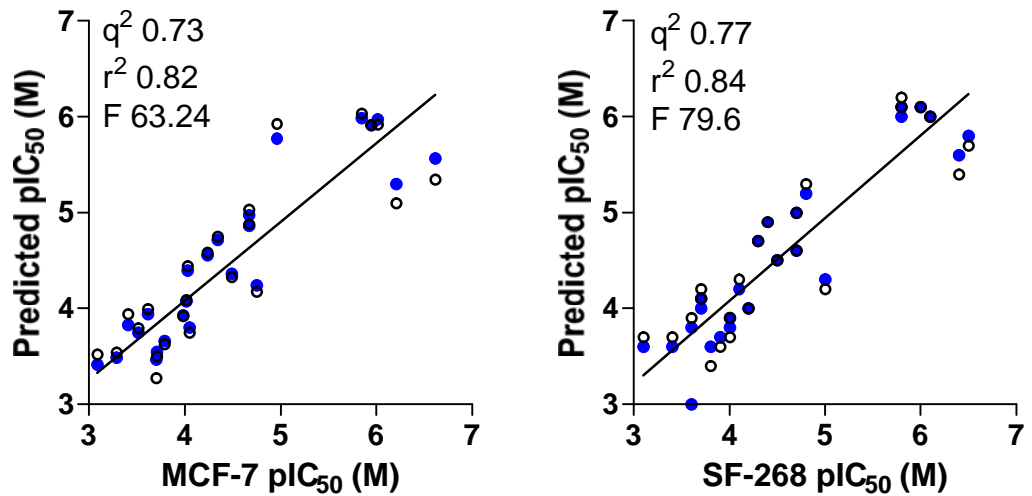


Figure S3: Hologram QSAR (HQSAR) results for MCF-7 and SF-268 cell lines, showing experimental versus predicted r^2 of 0.76 and 0.72 respectively.

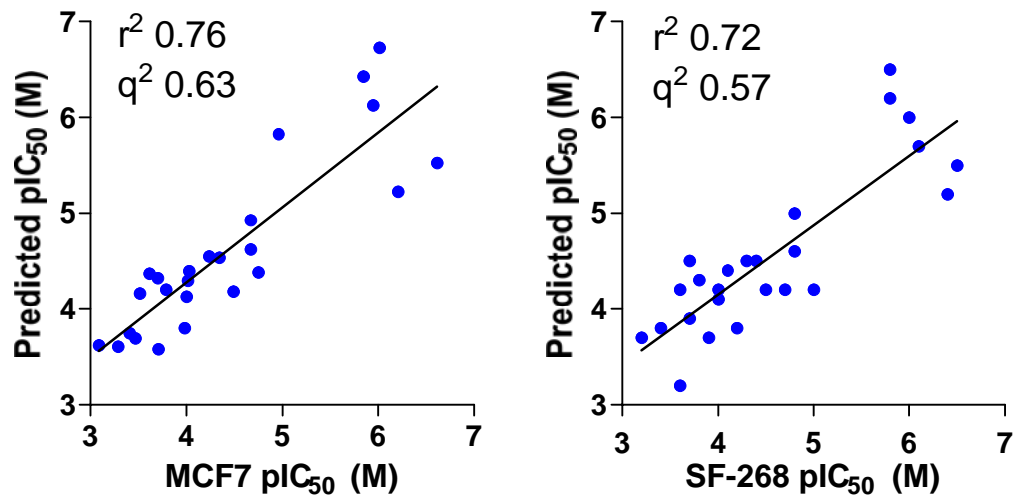
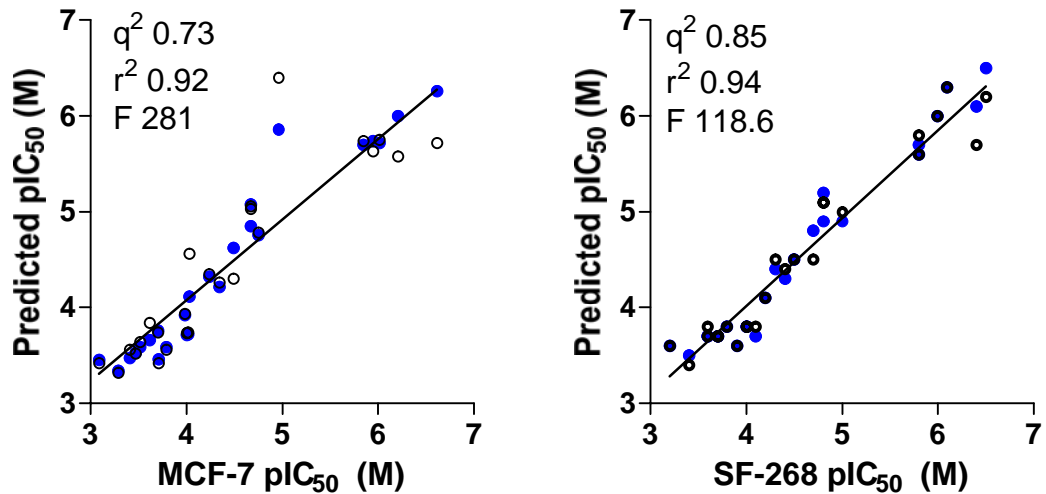


Figure S4: CoMSIA results for MCF-7 and SF-268 cell lines, $q^2 = 0.73$ and 0.94 respectively. ($pIC_{50} = -\log_{10}[IC_{50} M]$) (● = training set, ○ = test set).



Supporting Tables:

Table S1: Microanalysis

Cpd	Compound Name	% Carbon		% Hyrodgen		% Nitrogen	
		Theory	Found	Theory	Found	Theory	Found
14	2-[tetrahydrothiophenium-1-yl]-1,1-bisphosphonic acid	25.67	25.39	5.21	5	0	0
15	1-(2-Hydroxy-2,2-bis-phosphono-ethyl)-tetrahydro-thiophenium	24.66	24.73	4.83	4.81	0	0
16	1-(3-Hydroxy-3,3-bis-phosphono-propyl)-tetrahydro-thiophenium	27.46	26.9	5.27	5.21	0	0
17	1-(3-Hydroxy-3,3-bis-phosphono-propyl)-tetrahydro-thiopyranium	27.46	27.12	5.27	5.25	0	0
18	1-(3-Hydroxy-3,3-bis-phosphono-propyl)-tetrahydro-thiopyranium	29.18	28.66	5.82	5.49	0	0
19	1-(4-Hydroxy-4,4-bis-phosphono-butyl)-tetrahydro-thiophenium	29.34	28.79	5.76	5.21	0	0
20	(2-Hydroxy-2,2-bis-phosphono-ethyl)-methyl-(3-phenyl-propyl)-sulfonium	38.18	37.81	5.55	5.06	0	0
21	(2-Hydroxy-2,2-bis-phosphono-ethyl)-methyl-(3-phenoxy-propyl)-sulfonium	36.46	36.12	5.35	5.21	0	0
22	2-(phenylpentylmethylsulfonium-1-yl)ethylidene-1,1-bisphosphonic acid	42.97	42.9	6.44	6.27	0	0
23	(phenylbutylmethylsulfonium-1-yl)ethylidene-1,1-bisphosphonic acid	41.78	41.79	6.1	5.96	0	0
24	2-(methylphenylpropylsulfonium-1-yl)-ethylidene-1,1-bisphosphonic acid	39.67	39.91	5.83	5.62	0	0
25	(3-Hydroxy-3,3-bis-phosphono-propyl)-methyl-(3-phenyl-propyl)-sulfonium	39.7	39.64	5.89	5.64	0	0
26	(3-Hydroxy-3,3-bis-phosphono-propyl)-methyl-(3-phenoxy-propyl)-sulfonium	35.46	35.71	5.26	5.37	0	0
27	(3-Hydroxy-3,3-bis-phosphono-propyl)-methyl-phenethyl-sulfonium	35.13	34.67	5.16	5.09	0	0
28	1-(3-Hydroxy-3,3-bis-phosphono-propyl)-3-phenyl-tetrahydro-thiophenium	34.75	34.57	5.38	5.35	0	0
29	2-(S-methyl,S-4butyric acidphenyl-sulfonium-1-yl)ethylidene-1,1-bisphosphonic acid	44.06	44.24	6.31	6.2	0	0
30	2(methyldodecylsulfonium-1-yl)ethylidene-1,1-bisphosphonic acid	43.96	43.95	8.51	8.54	0	0
31	2-(methyldecylsulfonium-1-yl)ethylidene-1,1-bisphosphonic acid	40.9	40.58	8.08	7.76	0	0
32	2-(methyltetradecylsulfonium-1-yl)ethylidene-1,1-bisphosphonic acid	46.25	46.23	8.9	8.82	0	0
33	2-(methyltridecylsulfonium-1-yl)-1,1-bisphosphonic acid	43.85	43.6	8.79	8.46	0	0
34	2-(methylundecylsulfonium-1-yl)-1,1-bisphosphonic acid	41.17	41.32	8.39	8.09	0	0

35	2-(methylicosylsulfonium-1-yl)-1,1-bisphosphonic acid	50.11	50.02	9.22	9.44	0	0
36	2-(methyoctadecylsulfonium-1-yl)-1,1-bisphosphonic acid	46.11	45.88	8.4	8.81	0	0
37	2-(methylhexadecylsulfonium-1-yl)ethylidene-1,1-bisphosphonic acid	47.33	47.18	9.28	8.91	0	0
38	2-(methyloctylsulfonium-1-yl)ethylidien-1,1-bisphosphonic acid	37.93	37.77	7.52	7.58	0	0
40	(2-Hydroxy-2,2-bis-phosphono-ethyl)-methyl-propyl-sulfonium	18.98	18.7	4.94	4.56	0	0
41	2-(methylpropylsulfonium-1-yl)-ethylidene-1,1-bisphosphonic acid	25.9	25.54	5.8	5.74	0	0
42	(3-Hydroxy-3,3-bis-phosphono-propyl)-dimethyl-sulfonium	22.3	22.64	5.44	5.08	0	0
43	(2-Hydroxy-2,2-bis-phosphono-ethyl)-dimethyl-sulfonium	18.05	18.43	4.54	4.7	0	0
44	2-(methylarmylsulfonium-1-yl)ethylidene 1,1-bisphosphonic acid	30.13	29.81	6.76	6.34	0	0
46	(3-Hydroxy-3,3-bis-phosphono-propyl)-methyl-propyl-sulfonium	25.46	25.67	5.19	5.54	0	0

Table S2: Relationship between human FPPS inhibition and molecular diameter^c.

Cpd ^a	Human FPPS IC ₅₀ (μ M)	Human FPPS pIC ₅₀	
		(M) ^b	diameter ^c
43	1.03	6.0	5
42	9.00	5.0	6
41	0.53	6.3	7
44	1.08	6.0	9
38	0.36	6.4	12
31	0.24	6.6	14
30	0.26	6.6	16
32	8.47	5.1	18
36	7.45	5.1	20
37	45.60	4.3	20
36	7.45	5.1	22
35	27.40	4.6	24

^a Structures shown in Figures 1-3

^b pIC₅₀ = -log₁₀[IC₅₀ (M)]

^c Largest vertex eccentricity, Petitjean, M. J. Chem. Info., 32, 331-337, 1992

Table S3: Molecular Descriptor QSAR output for NCI-H460 model (summary of these results shown in Table 2 in the text).

QuaSAR-Model (PLS) : /Volumes/hudock/MOE/sulfonium/June2007/qsar_1_062107.mdb
 Sat Jul 21 11:51:43 2007

Activity Field : NCI_pIC50
 Weight Field :
 Condition Limit : 1e+06
 Component Limit : 0

Observations : 25
 Descriptors : 4
 Components Used : 4
 Condition Number : 597321.55

ROOT MEAN SQUARE ERROR (RMSE) : 0.39158
 CORRELATION COEFFICIENT (R2) : 0.84897
 CROSS-VALIDATED RMSE : 0.48660
 CROSS-VALIDATED R2 : 0.77138

ESTIMATED LINEAR MODEL

NCI_pIC50 =
 4.74682
 +0.32175 * b_Cont_Rot
 -0.01398 * SMR_VSA7
 -0.02456 * PEOE_VSA+2
 -0.00083 * weinerPath

ESTIMATED NORMALIZED LINEAR MODEL (SD = Standard Deviation)

NCI_pIC50 / SD(NCI_pIC50) =
 4.71101
 +1.82212 * b_Cont_Rot / SD(b_Cont_Rot)
 -0.36315 * SMR_VSA7 / SD(SMR_VSA7)
 -0.26633 * PEOE_VSA+2 / SD(PEOE_VSA+2)
 -0.90460 * weinerPath / SD(weinerPath)

RELATIVE IMPORTANCE OF DESCRIPTORS

1.000000 b_Cont_Rot
 0.199303 SMR_VSA7
 0.146166 PEOE_VSA+2
 0.496457 weinerPath

b_cont_Rot = Number of contiguous rotatable bonds.

SMR_VSA7 = Molar refractivity using the sub-divided molecular surface area method.

PEOE_VSA+2 = Partial Gasteiger charge using the sub-divided molecular surface area method.

weinerPath = Describes the compactness, branching and substitution of the molecule.

Table S4: Molecular Descriptor QSAR Results for MCF-7 cell line.

Cpd ^a			Molar			CV		
	Contiguous Rotatable Bonds	Weiner Path	Refractivity (SMR VSA7)	Gasteiger Charge (VSA+2)	MCF7 pIC ₅₀ (M)	Predicted pIC ₅₀ (M)	Predicted ^b pIC ₅₀ (M)	Residual
30	14	1818	110.91148	12.37335	6.6	5.6	5.3	1.3
31	12	1353	110.91148	12.37335	6.2	5.3	5.1	1.1
35	22	4718	110.91148	12.37335	6.0	6.0	5.9	0.1
37	18	3044	110.91148	12.37335	6.0	5.9	5.9	0.0
36	20	3821	110.91148	12.37335	5.8	6.0	6.0	-0.2
32	16	2379	110.91148	12.37335	5.0	5.8	5.9	-1.0
20	6	1154	77.585464	10.677375	4.8	4.2	4.2	0.6
22	9	1464	77.585464	12.37335	4.7	4.9	4.9	-0.2
38	10	976	110.91148	12.37335	4.7	5.0	5.0	-0.4
39	10	1261	110.91148	30.056063	4.5	4.4	4.3	0.2
23	8	1249	77.585464	12.37335	4.3	4.7	4.7	-0.4
24	7	1056	77.585464	12.37335	4.2	4.6	4.6	-0.3
15	2	397	45.894287	21.35475	4.1	3.8	3.7	0.3
21	7	1360	77.585464	10.677375	4.0	4.4	4.4	-0.4
14	3	351	45.894287	23.050724	4.0	4.1	4.1	-0.1
25	7	1362	77.585464	30.056063	4.0	3.9	3.9	0.1
40	4	413	110.91148	10.677375	3.8	3.7	3.6	0.2
16	3	499	45.894287	40.733437	3.7	3.5	3.5	0.2
43	2	270	109.27663	0	3.7	3.5	3.3	0.4
41	5	366	110.91148	12.37335	3.6	3.9	4.0	-0.4
17	2	478	45.894287	21.35475	3.5	3.7	3.8	-0.3
28	3	1129	58.534134	40.733437	3.5	3.0	2.7	0.8
45	7	756	110.91148	30.056063	3.4	3.8	3.9	-0.5
18	3	595	45.894287	40.733437	3.3	3.5	3.5	-0.3
46	5	516	110.91148	30.056063	3.1	3.4	3.5	-0.4

^a Structures shown in Figures 1-3^b Predicted values obtained from Leave-One-Out Cross Validation

Table S5: Molecular Descriptor QSAR output for MCF-7 model

QuaSAR-Model (PLS) : /Volumes/hudock/MOE/sulfonium/June2007/qsar_1_062107.mdb
Sat Jul 21 11:51:11 2007

Activity Field : MCF7_pIC50
Weight Field :
Condition Limit : 1e+06
Component Limit : 0

Observations : 25
Descriptors : 4
Components Used : 4
Condition Number : 597321.55

ROOT MEAN SQUARE ERROR (RMSE) : 0.41459
CORRELATION COEFFICIENT (R2) : 0.82124
CROSS-VALIDATED RMSE : 0.51079
CROSS-VALIDATED R2 : 0.73327

ESTIMATED LINEAR MODEL

MCF7_pIC50 =
4.67720
+0.28611 * b_Cont_Rot
-0.01473 * SMR_VSA7
-0.02422 * PEOE_VSA+2
-0.00065 * weinerPath

ESTIMATED NORMALIZED LINEAR MODEL (SD = Standard Deviation)

MCF7_pIC50 / SD(MCF7_pIC50) =
4.76983
+1.66491 * b_Cont_Rot / SD(b_Cont_Rot)
-0.39320 * SMR_VSA7 / SD(SMR_VSA7)
-0.26986 * PEOE_VSA+2 / SD(PEOE_VSA+2)
-0.72485 * weinerPath / SD(weinerPath)

RELATIVE IMPORTANCE OF DESCRIPTORS

1.000000 b_Cont_Rot
0.236166 SMR_VSA7
0.162089 PEOE_VSA+2
0.435367 weinerPath

b_cont_Rot = Number of contiguous rotatable bonds.

SMR_VSA7 = Molar refractivity using the sub-divided molecular surface area method.

PEOE_VSA+2 = Partial Gasteiger charge using the sub-divided molecular surface area method.

weinerPath = Describes the compactness, branching and substitution of the molecule.

Table S6: Molecular Descriptor QSAR Results for SF-268 cell line.

Cpd ^a	Contiguous Rotatable Bonds	Weiner Path	Molar		SF-268	Predicted	CV		Residual
			Refractivity (SMR VSA7)	Gasteiger Charge (VSA+2)			pIC ₅₀ (M)	Predicted ^b	
30	14	1818	110.91148	12.37335	6.5	5.8	5.7	0.9	
31	12	1353	110.91148	12.37335	6.4	5.6	5.4	1.1	
32	16	2379	110.91148	12.37335	6.1	6	6	0.1	
37	18	3044	110.91148	12.37335	6	6.1	6.1	-0.1	
35	22	4718	110.91148	12.37335	5.8	6	6.1	-0.3	
36	20	3821	110.91148	12.37335	5.8	6.1	6.2	-0.4	
20	6	1154	77.585464	10.677375	5	4.3	4.2	0.7	
38	10	976	110.91148	12.37335	4.8	5.2	5.3	-0.5	
22	9	1464	77.585464	12.37335	4.7	5	5	-0.3	
39	10	1261	110.91148	30.056063	4.7	4.6	4.6	0.1	
21	7	1360	77.585464	10.677375	4.5	4.5	4.5	0	
23	8	1249	77.585464	12.37335	4.4	4.9	4.9	-0.5	
24	7	1056	77.585464	12.37335	4.3	4.7	4.7	-0.4	
25	7	1362	77.585464	30.056063	4.2	4	4	0.2	
14	3	351	45.894287	23.050724	4.1	4.2	4.3	-0.2	
15	2	397	45.894287	21.35475	4	3.9	3.9	0.1	
40	4	413	110.91148	10.677375	4	3.8	3.7	0.3	
16	3	499	45.894287	40.733437	3.9	3.7	3.6	0.3	
43	2	270	109.27663	0	3.8	3.6	3.4	0.4	
41	5	366	110.91148	12.37335	3.7	4.1	4.2	-0.6	
45	7	756	110.91148	30.056063	3.7	4	4.1	-0.4	
17	2	478	45.894287	21.35475	3.6	3.8	3.9	-0.3	
28	3	1129	58.534134	40.733437	3.6	3	2.7	0.9	
18	3	595	45.894287	40.733437	3.4	3.6	3.7	-0.3	
46	5	516	110.91148	30.056063	3.1	3.6	3.7	-0.6	

^a Structures shown in Figures 1-3^b Predicted values obtained from Leave-One-Out Cross Validation

Table S7: Molecular Descriptor QSAR output for SF-268 model

QuaSAR-Model (PLS) : /Volumes/hudock/MOE/sulfonium/June2007/qsar_1_062107.mdb
Sat Jul 21 11:52:20 2007

Activity Field : SF268_pIC50
Weight Field :
Condition Limit : 1e+06
Component Limit : 0

Observations : 25
Descriptors : 4
Components Used : 4
Condition Number : 597321.55

ROOT MEAN SQUARE ERROR (RMSE) : 0.38182
CORRELATION COEFFICIENT (R2) : 0.84820
CROSS-VALIDATED RMSE : 0.47782
CROSS-VALIDATED R2 : 0.76793

ESTIMATED LINEAR MODEL

SF268_pIC50 =
4.76774
+0.32257 * b_Cont_Rot
-0.01496 * SMR_VSA7
-0.02305 * PEOE_VSA+2
-0.00084 * weinerPath

ESTIMATED NORMALIZED LINEAR MODEL (SD = Standard Deviation)

SF268_pIC50 / SD(SF268_pIC50) =
4.86504
+1.87817 * b_Cont_Rot / SD(b_Cont_Rot)
-0.39958 * SMR_VSA7 / SD(SMR_VSA7)
-0.25704 * PEOE_VSA+2 / SD(PEOE_VSA+2)
-0.93930 * weinerPath / SD(weinerPath)

RELATIVE IMPORTANCE OF DESCRIPTORS

1.000000 b_Cont_Rot
0.212750 SMR_VSA7
0.136858 PEOE_VSA+2
0.500113 weinerPath

b_cont_Rot = Number of contiguous rotatable bonds.

SMR_VSA7 = Molar refractivity using the sub-divided molecular surface area method.

PEOE_VSA+2 = Partial Gasteiger charge using the sub-divided molecular surface area method.

weinerPath = Describes the compactness, branching and substitution of the molecule.

Table S8: Hologram (HQSAR) results and output for MCF-7, NCI-H460 and SF-268 cell lines. Average experiment vs. predicted $r^2 = 0.76$, $q^2 = 0.6$.

Cpd	NCI-H460			MCF-7			SF-268		
	pIC ₅₀ (M)	Predicted pIC ₅₀ (M)	Residual	pIC ₅₀ (M)	Predicted pIC ₅₀ (M)	Residual	pIC ₅₀ (M)	Predicted pIC ₅₀ (M)	Residual
30	6.7	5.5	1.2	6.6	5.4	1.2	6.5	5.5	1.1
31	6.5	5.2	1.3	6.2	5.1	1.1	6.4	5.2	1.2
32	6.3	5.7	0.6	5.0	5.7	-0.8	6.1	5.7	0.3
35	5.9	6.6	-0.6	6.0	6.6	-0.6	5.8	6.5	-0.7
36	5.9	6.3	-0.4	5.9	6.3	-0.5	5.8	6.2	-0.5
37	5.9	6.0	-0.2	6.0	6.0	-0.1	6.0	6.0	0.0
38	4.9	4.9	0.0	4.7	4.8	-0.2	4.8	5.0	-0.1
20	4.9	4.3	0.5	4.8	4.4	0.3	5.0	4.2	0.8
21	4.8	4.3	0.5	4.0	4.3	-0.3	4.5	4.2	0.2
22	4.6	4.7	0.0	4.7	4.6	0.1	4.8	4.6	0.2
39	4.6	4.2	0.4	4.5	4.2	0.3	4.7	4.2	0.5
23	4.3	4.6	-0.3	4.3	4.5	-0.2	4.4	4.5	-0.1
24	4.3	4.6	-0.3	4.2	4.5	-0.3	4.3	4.5	-0.2
25	4.2	3.9	0.3	4.0	3.9	0.1	4.2	3.8	0.4
40	4.1	4.1	0.0	3.8	4.2	-0.4	4.0	4.2	-0.2
14	4.1	4.3	-0.2	4.0	4.2	-0.2	4.1	4.4	-0.3
41	4.0	4.4	-0.4	3.6	4.3	-0.7	3.7	4.5	-0.8
15	3.9	4.0	-0.1	4.0	4.1	-0.1	4.0	4.1	-0.1
16	3.8	3.6	0.2	3.7	3.6	0.1	3.9	3.7	0.2
43	3.7	4.2	-0.5	3.7	4.3	-0.6	3.8	4.3	-0.5
45	3.7	3.8	-0.1	3.4	3.8	-0.3	3.7	3.9	-0.2
17	3.7	4.1	-0.4	3.5	4.1	-0.6	3.6	4.2	-0.6
28	3.6	3.3	0.3	3.5	3.6	-0.2	3.6	3.2	0.3
18	3.5	3.7	-0.2	3.3	3.6	-0.3	3.4	3.8	-0.4
46	3.1	3.7	-0.6	3.1	3.6	-0.5	3.2	3.7	-0.6
	q2	0.6		q2	0.6		q2	0.57	
	r2	0.76		r2	0.76		r2	0.75	
Length	151		Length	353		Length	353		

	N	3		N	3		N	3
--	---	---	--	---	---	--	---	---

Table S9: CoMSIA output for NCI-H460 model (full table shown in the main text).

Maximum common substructure alignment:

Regression Equation(s)

Use COMFA FIELD RETRIEVE/LIST/GRAPH or EVA RETRIEVE/LIST/GRAPH

ComFA/EVA coefficients.

All columns are COMFA.

Relative Contributions

#	Norm.Coeff.	Fraction
-		
1 COMSIA_ST (1368 vars)	0.538	0.234
2 COMSIA_EL (1368 vars)	0.087	0.038
3 COMSIA_HY (1368 vars)	0.872	0.380
4 COMSIA_DO (1368 vars)	0.436	0.190
5 COMSIA_AC (1368 vars)	0.364	0.159

Input Selections: PLS Analysis

Minimum Sigma to use Column: 0.0000 Missing Values: COLUMN_MEAN_DEFAULT

Row Weighting: SAME_WEIGHTS_FOR_ALL

Neither BOOTSTRAPPED nor CROSSVALIDATED

COMPONENTS: 4

Scaling: COMFA_STANDARD Intercept forced through 0.0: NO

NIPALS: (Max Iter = 100; EPS = 0.000100)

Target (Y) Variable(s):

2: NCI_pIC50

Explanatory (X) Variable(s): (Actual terms: 6840 requested, 6372 used)

4: COMSIA_ST 5: COMSIA_EL 6: COMSIA_HY

7: COMSIA_DO 8: COMSIA_AC

Rows in Analysis: (25 rows)

1: 546	2: 569	3: 572
4: 575	5: 576	6: 584
7: 585	8: 589	9: 594
10: 682	11: 683	12: 685
13: 686	14: 687	15: 688
16: 689	17: 690	18: 694
19: 695	20: 696	21: 697
22: 527	23: 580	24: 547
25: 574		

Summary output

Standard Error of Estimate 0.273

R squared 0.941

F values (n1= 4, n2=20) 80.178

Prob.of R2=0 (n1= 4, n2=20) 0.000

Feature-based alignment:

Regression Equation(s)

Use COMFA FIELD RETRIEVE/LIST/GRAPH or EVA RETRIEVE/LIST/GRAPH

ComFA/EVA coefficients.

All columns are COMFA.

Relative Contributions

#	Norm.Coeff.	Fraction
-		
1 COMSIA_ST (1872 vars)	0.699	0.330
2 COMSIA_EL (1872 vars)	0.081	0.038
3 COMSIA_HY (1872 vars)	1.100	0.519
4 COMSIA_DO (1872 vars)	0.183	0.086
5 COMSIA_AC (1872 vars)	0.056	0.026

Input Selections: PLS Analysis

Minimum Sigma to use Column: 0.0000 Missing Values: COLUMN_MEAN_DEFAULT

Row Weighting: SAME_WEIGHTS_FOR_ALL
Neither BOOTSTRAPPED nor CROSSVALIDATED
COMPONENTS: 4
Scaling: COMFA_STANDARD Intercept forced through 0.0: NO
NIPALS: (Max Iter = 100; EPS = 0.000100)
Target (Y) Variable(s):
2: NCI_pIC50
Explanatory (X) Variable(s): (Actual terms: 9360 requested, 8830 used)
4: COMSIA_ST 5: COMSIA_EL 6: COMSIA_HY
7: COMSIA_DO 8: COMSIA_AC
Rows in Analysis: (25 rows)
1: 527 2: 546 3: 569
4: 572 5: 575 6: 576
7: 580 8: 584 9: 585
10: 589 11: 594 12: 682
13: 683 14: 685 15: 686
16: 687 17: 688 18: 689
19: 690 20: 694 21: 695
22: 696 23: 697 24: 547
25: 574

Summary output
Standard Error of Estimate 0.216
R squared 0.963
F values (n1= 4, n2=20) 131.391
Prob.of R2=0 (n1= 4, n2=20) 0.000

Table S10: CoMSIA QSAR results for MCF-7 cell line.

Cpd	MCF-7 Experimental Activity		CoMSIA pIC ₅₀ Predictions								
	IC ₅₀ (μM)	pIC ₅₀ (M)	Training Set	Test Sets					Pred	Residual	
				1	2	3	4	5			
30	0.24	6.6	6.3	6.5	6.3	6.0	5.7	6.3	5.7	-0.54	
31	0.62	6.2	6.0	6.1	6.1	5.6	5.8	6.0	5.6	-0.42	
35	0.95	6.0	5.7	5.8	5.7	5.8	5.9	5.6	5.7	0.03	
37	1.12	6.0	5.7	6.1	5.7	5.8	5.7	5.6	5.6	-0.11	
36	1.41	5.9	5.7	5.9	5.7	5.8	5.8	5.6	5.7	0.04	
32	10.96	5.0	5.9	6.4	5.9	5.8	5.5	5.8	6.4	0.54	
20	17.78	4.8	4.7	4.7	4.7	4.9	4.8	4.8	4.8	0.03	
38	21.38	4.7	5.1	5.1	5.1	4.9	5.1	5.1	5.1	-0.02	
22	21.38	4.7	4.8	4.8	4.8	4.8	5.0	4.8	5.0	0.18	
39	32.36	4.5	4.6	4.5	4.3	4.6	4.7	4.6	4.3	-0.32	
23	45.71	4.3	4.2	4.2	4.2	4.3	4.3	4.2	4.3	0.05	
24	57.54	4.2	4.3	4.3	4.3	4.5	4.4	4.3	4.4	0.03	
21	93.33	4.0	4.1	4.1	4.1	4.6	4.1	4.1	4.6	0.45	
14	95.50	4.0	3.7	3.8	3.7	3.7	3.8	3.7	3.7	0.02	
15	100.00	4.0	3.7	3.7	3.7	3.8	3.7	3.7	3.7	0.02	
25	104.71	4.0	3.9	3.9	4.0	3.9	3.9	3.9	3.9	0.01	
40	162.18	3.8	3.6	3.6	3.6	3.7	3.6	3.6	3.6	-0.03	
16	194.98	3.7	3.5	3.5	3.4	3.4	3.4	3.5	3.4	-0.04	
43	199.53	3.7	3.8	3.8	3.7	3.7	3.8	3.7	3.7	-0.02	
41	239.88	3.6	3.7	3.8	3.7	3.6	3.7	3.7	3.8	0.18	
17	302.00	3.5	3.6	3.6	3.6	3.8	3.6	3.6	3.6	0.05	
28	338.84	3.5	3.5	3.5	3.6	3.5	3.5	3.5	3.5	-0.01	
45	389.05	3.4	3.5	3.5	3.4	3.4	3.4	3.6	3.6	0.10	
18	512.86	3.3	3.3	3.3	3.3	3.3	3.3	3.3	3.3	-0.02	
46	812.83	3.1	3.4	3.5	3.4	3.3	3.4	3.5	3.4	-0.03	
		q ²	0.73	0.75	0.73	0.75	0.76	0.7			
		R ²	0.93	0.83	0.9	0.841	0.845	0.81			
		F test	61.789	5	60	53	54.3	41.7			

N	4	4	4	4	4	4
n	25	23	23	23	23	23

Table S11: CoMSIA output for MCF-7 model.

Maximum common substructure alignment:

Regression Equation(s)

Use COMFA FIELD RETRIEVE/LIST/GRAPH or EVA RETRIEVE/LIST/GRAPH

ComFA/EVA coefficients.

All columns are COMFA.

Relative Contributions

#	Norm.Coeff.	Fraction
-		
1 COMSIA_ST (1368 vars)	0.513	0.205
2 COMSIA_EL (1368 vars)	0.099	0.040
3 COMSIA_HY (1368 vars)	0.855	0.342
4 COMSIA_DO (1368 vars)	0.647	0.259
5 COMSIA_AC (1368 vars)	0.384	0.154

Input Selections: PLS Analysis

Minimum Sigma to use Column: 0.0000 Missing Values: COLUMN_MEAN_DEFAULT

Row Weighting: SAME_WEIGHTS_FOR_ALL

Neither BOOTSTRAPPED nor CROSSVALIDATED

COMPONENTS: 4

Scaling: COMFA_STANDARD Intercept forced through 0.0: NO

NIPALS: (Max Iter = 100; EPS = 0.000100)

Target (Y) Variable(s):

1: MCF7_pIC50

Explanatory (X) Variable(s): (Actual terms: 6840 requested, 6372 used)

4: COMSIA_ST	5: COMSIA_EL	6: COMSIA_HY
7: COMSIA_DO	8: COMSIA_AC	

Rows in Analysis: (25 rows)

1: 546	2: 569	3: 572
4: 575	5: 576	6: 584
7: 585	8: 589	9: 594
10: 682	11: 683	12: 685
13: 686	14: 687	15: 688
16: 689	17: 690	18: 694
19: 695	20: 696	21: 697
22: 527	23: 580	24: 547
25: 574		

Summary output

Standard Error of Estimate 0.326

R squared 0.912

F values (n1= 4, n2=20) 51.682

Prob.of R2=0 (n1= 4, n2=20) 0.000

Feature-based alignment:

Regression Equation(s)

Use COMFA FIELD RETRIEVE/LIST/GRAPH or EVA RETRIEVE/LIST/GRAPH

ComFA/EVA coefficients.

All columns are COMFA.

Relative Contributions

#	Norm.Coeff.	Fraction
-		
1 COMSIA_ST (1872 vars)	0.652	0.306
2 COMSIA_EL (1872 vars)	0.072	0.034
3 COMSIA_HY (1872 vars)	1.029	0.484
4 COMSIA_DO (1872 vars)	0.313	0.147
5 COMSIA_AC (1872 vars)	0.062	0.029

Input Selections: PLS Analysis

Minimum Sigma to use Column: 0.0000 Missing Values: COLUMN_MEAN_DEFAULT
 Row Weighting: SAME_WEIGHTS_FOR_ALL
 Neither BOOTSTRAPPED nor CROSSVALIDATED
 COMPONENTS: 4
 Scaling: COMFA_STANDARD Intercept forced through 0.0: NO
 NIPALS: (Max Iter = 100; EPS = 0.000100)
 Target (Y) Variable(s):
 1: MCF7_pIC50
 Explanatory (X) Variable(s): (Actual terms: 9360 requested, 8830 used)
 4: COMSIA_ST 5: COMSIA_EL 6: COMSIA_HY
 7: COMSIA_DO 8: COMSIA_AC
 Rows in Analysis: (25 rows)
 1: 527 2: 546 3: 569
 4: 572 5: 575 6: 576
 7: 580 8: 584 9: 585
 10: 589 11: 594 12: 682
 13: 683 14: 685 15: 686
 16: 687 17: 688 18: 689
 19: 690 20: 694 21: 695
 22: 696 23: 697 24: 547
 25: 574

Summary output
 Standard Error of Estimate 0.300
 R squared 0.925
 F values (n1= 4, n2=20) 61.789
 Prob.of R2=0 (n1= 4, n2=20) 0.000

Table S12: CoMSIA QSAR results for SF-268 cell line.

Cpd	SF-268 Experimental Activity		Training Set	CoMSIA pIC ₅₀ Predictions							
	IC ₅₀ (μM)	pIC ₅₀ (M)		Test Sets					Pred	Residual	
				1	2	3	4	5			
30	0.32	6.5	6.5	6.6	6.5	6.2	6.2	6.5	6.2	-0.27	
31	0.32	6.4	6.1	6.2	6.1	5.7	6.0	6.1	5.7	-0.39	
32	0.32	6.1	6.3	6.4	6.4	6.2	6.2	6.4	6.3	-0.02	
37	0.32	6.0	6.0	6.1	6.0	6.0	6.0	6.0	6.0	-0.02	
35	0.32	5.8	5.6	5.6	5.6	5.6	5.6	5.6	5.6	0.02	
36	0.32	5.8	5.7	5.8	5.7	5.8	5.8	5.7	5.8	0.07	
20	0.32	5.0	4.9	5.0	4.9	5.0	5.0	4.9	5.0	0.02	
38	0.32	4.8	5.2	5.2	5.1	5.0	5.2	5.2	5.1	-0.01	
22	0.32	4.8	4.9	4.9	4.8	4.9	5.1	4.9	5.1	0.19	
39	0.32	4.7	4.8	4.8	4.5	4.7	4.9	4.7	4.5	-0.29	
21	0.32	4.5	4.5	4.5	4.4	4.6	4.5	4.5	4.5	0.03	
23	0.32	4.4	4.3	4.3	4.4	4.4	4.4	4.3	4.4	0.02	
24	0.32	4.3	4.4	4.4	4.4	4.5	4.5	4.4	4.5	0.09	
25	0.32	4.2	4.1	4.1	4.1	4.1	4.1	4.1	4.1	0.01	
14	0.32	4.1	3.7	3.8	3.7	3.7	3.8	3.8	3.8	0.01	
40	0.32	4.0	3.8	3.8	3.7	3.9	3.8	3.8	3.8	0.01	
15	0.32	4.0	3.8	3.8	3.8	3.8	3.7	3.8	3.8	0.05	
16	0.32	3.9	3.6	3.6	3.6	3.5	3.6	3.6	3.6	-0.03	
43	0.32	3.8	3.8	3.9	3.8	3.8	3.8	3.8	3.8	-0.02	
45	0.32	3.7	3.7	3.7	3.7	3.7	3.7	3.7	3.7	0.00	
41	0.32	3.7	3.7	3.8	3.7	3.7	3.7	3.7	3.7	0.03	
17	0.32	3.6	3.7	3.7	3.7	3.9	3.7	3.8	3.8	0.02	
28	0.32	3.6	3.7	3.7	3.7	3.7	3.6	3.7	3.7	0.02	
18	0.32	3.4	3.5	3.4	3.4	3.4	3.4	3.5	3.4	-0.01	
46	0.32	3.2	3.6	3.6	3.5	3.5	3.6	3.6	3.6	-0.03	
		q ²	0.85	0.78	0.844	0.82	0.82	0.82			
		R ²	0.96	0.95	0.96	0.96	0.96	0.96			

F test	118.6	84.4	119.7	104.7	110.2	97.7
N	4	4	4	4	4	4
n	25	23	23	23	23	23

Table S13: CoMSIA output for SF-268 model.

Maximum common substructure alignment:

Regression Equation(s)

Use COMFA FIELD RETRIEVE/LIST/GRAPH or EVA RETRIEVE/LIST/GRAPH

ComFA/EVA coefficients.

All columns are COMFA.

Relative Contributions

#	Norm.Coeff.	Fraction
-		
1 COMSIA_ST (1368 vars)	0.557	0.241
2 COMSIA_EL (1368 vars)	0.095	0.041
3 COMSIA_HY (1368 vars)	0.882	0.382
4 COMSIA_DO (1368 vars)	0.429	0.186
5 COMSIA_AC (1368 vars)	0.345	0.150

Input Selections: PLS Analysis

Minimum Sigma to use Column: 0.0000 Missing Values: COLUMN_MEAN_DEFAULT

Row Weighting: SAME_WEIGHTS_FOR_ALL

Neither BOOTSTRAPPED nor CROSSVALIDATED

COMPONENTS: 4

Scaling: COMFA_STANDARD Intercept forced through 0.0: NO

NIPALS: (Max Iter = 100; EPS = 0.000100)

Target (Y) Variable(s):

3: SF268_pIC50

Explanatory (X) Variable(s): (Actual terms: 6840 requested, 6372 used)

4: COMSIA_ST	5: COMSIA_EL	6: COMSIA_HY
7: COMSIA_DO	8: COMSIA_AC	

Rows in Analysis: (25 rows)

1: 546	2: 569	3: 572
4: 575	5: 576	6: 584
7: 585	8: 589	9: 594
10: 682	11: 683	12: 685
13: 686	14: 687	15: 688
16: 689	17: 690	18: 694
19: 695	20: 696	21: 697
22: 527	23: 580	24: 547
25: 574		

Summary output

Standard Error of Estimate 0.267

R squared 0.940

F values (n1= 4, n2=20) 79.023

Prob.of R2=0 (n1= 4, n2=20) 0.000

Feature-based alignment:

Regression Equation(s)

Use COMFA FIELD RETRIEVE/LIST/GRAPH or EVA RETRIEVE/LIST/GRAPH

ComFA/EVA coefficients.

All columns are COMFA.

Relative Contributions

#	Norm.Coeff.	Fraction
-		
1 COMSIA_ST (1872 vars)	0.678	0.320
2 COMSIA_EL (1872 vars)	0.077	0.037
3 COMSIA_HY (1872 vars)	1.064	0.502
4 COMSIA_DO (1872 vars)	0.240	0.113
5 COMSIA_AC (1872 vars)	0.060	0.028

Input Selections: PLS Analysis

Minimum Sigma to use Column: 0.0000 Missing Values: COLUMN_MEAN_DEFAULT
Row Weighting: SAME_WEIGHTS_FOR_ALL
Neither BOOTSTRAPPED nor CROSSVALIDATED
COMPONENTS: 4
Scaling: COMFA_STANDARD Intercept forced through 0.0: NO
NIPALS: (Max Iter = 100; EPS = 0.000100)
Target (Y) Variable(s):
3: SF268_pIC50
Explanatory (X) Variable(s): (Actual terms: 9360 requested, 8830 used)
4: COMSIA_ST 5: COMSIA_EL 6: COMSIA_HY
7: COMSIA_DO 8: COMSIA_AC
Rows in Analysis: (25 rows)
1: 527 2: 546 3: 569
4: 572 5: 575 6: 576
7: 580 8: 584 9: 585
10: 589 11: 594 12: 682
13: 683 14: 685 15: 686
16: 687 17: 688 18: 689
19: 690 20: 694 21: 695
22: 696 23: 697 24: 547
25: 574

Summary output
Standard Error of Estimate 0.220
R squared 0.960
F values (n1= 4, n2=20) 118.549
Prob.of R2=0 (n1= 4, n2=20) 0.000

References:

1. Labute, P., A widely applicable set of descriptors. *J. Mol. Graph. Modelling* **2000**, 18, (4-5), 464-477.
2. Guba, W., Descriptors and Representation of Chemicals. In *Predictive Toxicology*, C, H., Ed. Taylor & Francis: CRC London, 2005; pp 11-36.
3. Kavanagh, K. L.; Guo, K.; Dunford, J. E.; Wu, X.; Knapp, S.; Ebetino, F. H.; Rogers, M. J.; Russell, R. G.; Oppermann, U., The molecular mechanism of nitrogen-containing bisphosphonates as antiosteoporosis drugs. *Proc. Natl. Acad. Sci. U.S.A.* **2006**, 103, (20), 7829-34.
4. Mao, J.; Gao, Y. G.; Odeh, S.; Robinson, H.; Montalvetti, A.; Docampo, R.; Oldfield, E., Crystallization and Preliminary X-ray Diffraction Study of the Farnesyl Diphosphate Synthase from *Trypanosoma brucei*. *Acta Crystallogr. D Biol. Crystallogr.* **2004**, 60, (Pt 10), 1863-6.
5. Navaza, J., AMoRe: an automated package for molecular replacement. *Acta Crystallogr. Sect. A* **1994**, 50, 157-163.
6. Sheldrick, G.; Schneider, T., SHELLXL: High Resolution Refinement. *Methods in Enzymology* **1997**, 277, 319-343.
7. Jones, T. A.; Zou, J. Y.; Cowan, S. W.; Kjeldgaard, M., Improved methods for building protein models in electron density maps and the location of errors in these models. *Acta Crystallogr. Sect. A* **1991**, 47, 110-119.
8. Mao, J.; Mukherjee, S.; Zhang, Y.; Cao, R.; Sanders, J. M.; Song, Y.; Zhang, Y.; Meints, G. A.; Gao, Y. G.; Mukkamala, D.; Hudock, M. P.; Oldfield, E., Solid-state NMR, crystallographic, and computational investigation of bisphosphonates and farnesyl diphosphate synthase-bisphosphonate complexes. *J. Am. Chem. Soc.* **2006**, 128, (45), 14485-97.
9. Brunger, A. T.; Adams, P. D.; Clore, G. M.; DeLano, W. L.; Gros, P.; Grosse-Kunstleve, R. W.; Jiang, J. S.; Kuszewski, J.; Nilges, M.; Pannu, N. S.; Read, R. J.; Rice, L. M.; Simonson, T.; Warren, G. L., Crystallography & NMR system: A new software suite for macromolecular structure determination. *Acta Crystallogr. D Biol. Crystallogr.* **1998**, 54, (Pt 5), 905-21.
10. Emsley, P.; Cowtan, K., Coot: model-building tools for molecular graphics. *Acta Crystallogr. D Biol. Crystallogr.* **2004**, 60, (Pt 12 Pt 1), 2126-32.